

# Tests of high-strength concrete interior beam-column-joint subassemblages

Koji Oka

*Ohmoto-gumi Co., Ltd, Tokyo, Japan*

Hitoshi Shiohara

*Building Research Institute, Tsukuba, Japan*

**ABSTRACT :** In order to evaluate the availability of current design provisions in high seismic regions for interior beam-column-joints using high strength concrete, Eleven 1/2.5 scale interior beam column-joint subassemblages were made and were subjected to statically cyclic loading to failure, maintaining constant axial load on the column. The parameter of the specimens includes (1) concrete compressive strength (40 MPa - 80 MPa), (2) yield strength of longitudinal reinforcing steel (350 MPa - 1,400 MPa), (3) amount of beam longitudinal reinforcement, and (4) with or without the slab and transverse beam. The behavior of the specimens such as maximum horizontal joint shear, failure mode, and hysteretic characteristics, were compared with those of control specimens made of normal strength materials.

## 1. INTRODUCTION

Usage of super-plasticizer makes it realistic to utilize high-strength concrete in practice for cast-in-place concrete buildings, which will probably enable structural designer to design more slender reinforced concrete member. High strength mild steel reinforcing bar is also promising for use if high strength concrete is combined with high strength concrete, to prevent from congested detail of reinforcing bar in more slender member. However it is uncertain whether or not the current structural design code is available, because they are not intended to be used for structure using high strength material by extrapolation of existing provisions in the code. Current beam-column-joint design provisions for high seismic zone are based on many tests conducted on specimens constructed with conventional strength materials. Few tests of earthquake resisting performance of beam-column-subassemblages using high strength material is reported except a recent paper by Guimaraes et al. (1992). Thus, an experimental research program was planned to investigate the earthquake resisting performance of beam-column connection. Eleven 1/2.5 scale interior beam-column-joint subassemblages were tested at Building Research Institute since 1989. This paper reports the selected test results including maximum horizontal joint shear, failure mode, and hysteretic characteristics, which are compared with those of control specimens made of conventional strength materials.

## 2. TEST PROGRAM

### 2.1 Parameters

Eleven 1/2.5 scale cruciform beam-column-joint subassemblages were made using high strength concrete and/or high strength reinforcing steel. Table 1 lists the design parameters of the specimens, including combination of material strengths, nominal joint shear stress

Table 1 : Design Parameters of Specimens

	Concrete Strength (MPa)	Steel Strength (MPa)	Nominal joint shear (MPa)	Development length nominal diameter
J-1	80	700	14.7	23.6
J-2	80	1,400	29.5	23.1
J-3	80	1,400	29.5	23.1
J-4	80	500	13.2	23.6
J-5	80	800	16.8	23.6
J-6	80	700	14.7	23.6
J-7	80	700	11.0	23.6
J-8	80	350	16.5	15.7
J-9	80	700	14.4	23.6
J-10	40	700	14.7	23.6
J-11	40	350	16.5	15.7

Table 2 : Reinforcement Arrangements

	BEAM		COLUMN		AXIAL LOAD
	size	top bars	bottom bars	size bars	
J-1	D13	9	7	D13 24	834
J-2	U13	8	8	U13 24	834
J-3	U13	8	8	U13 24	834
J-4	D13	10	10	D13 24	834
J-5	D13	9	7	D13 24	834
J-6	D13	9	7	D13 24	834
J-7	D13	7	5	D13 24	834
J-8	D19	9	7	D19 24	834
J-9	D13	7	7	D13 24	834
J-10	D13	9	7	D13 24	417
J-11	D19	9	7	D19 24	417

and development length of beam longitudinal reinforcement through joint. The parameters of the specimens include; (1) concrete compressive strength (40 MPa and 80 MPa), (2) yield strength of longitudinal reinforcing steel (350 MPa - 1,400 MPa), (3) amount of beam longitudinal reinforcement, and (4) with or without the slab and transverse beam. Table 2 lists the reinforcement arrangement of the specimens. All of the specimens were designed to cause beam side-sway mechanism considering overstrength of beams.

## 2.2 Geometry of Specimens and Material Properties

Geometry of two specimens J-1 and J-9 are shown in Fig. 1. The other specimens had the same geometry with J-1. The beams were 24 cm wide and 30 cm deep, and the column had a 30 cm square cross section in common. The specimen J-9 had the common dimensions but it also had a 6 cm thick slab and transverse beams.

Figure 2 shows the geometry of the sections and Ta-

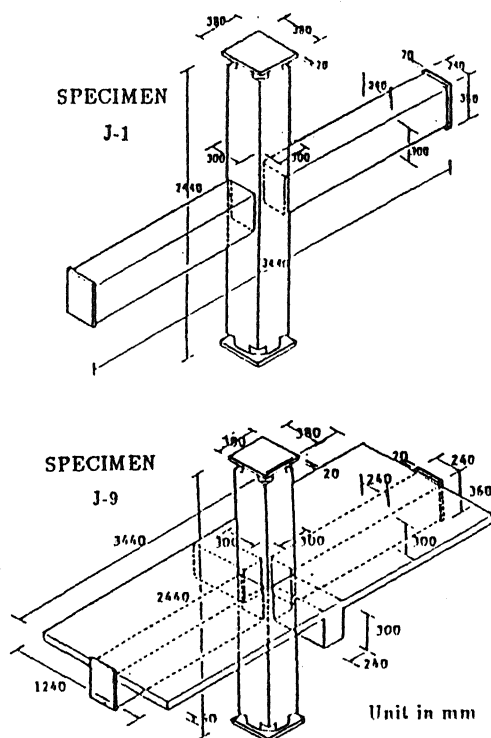
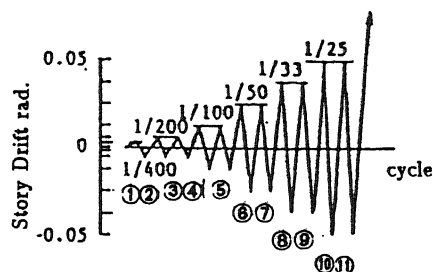
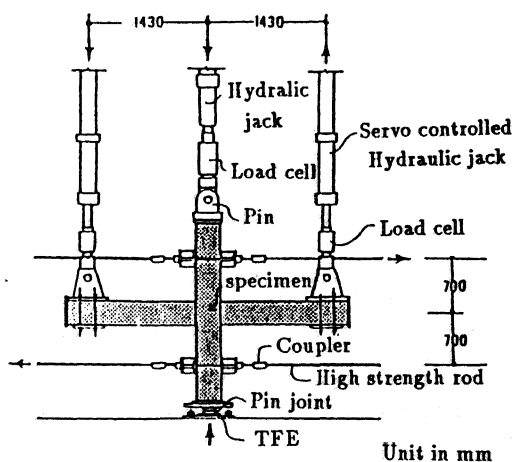
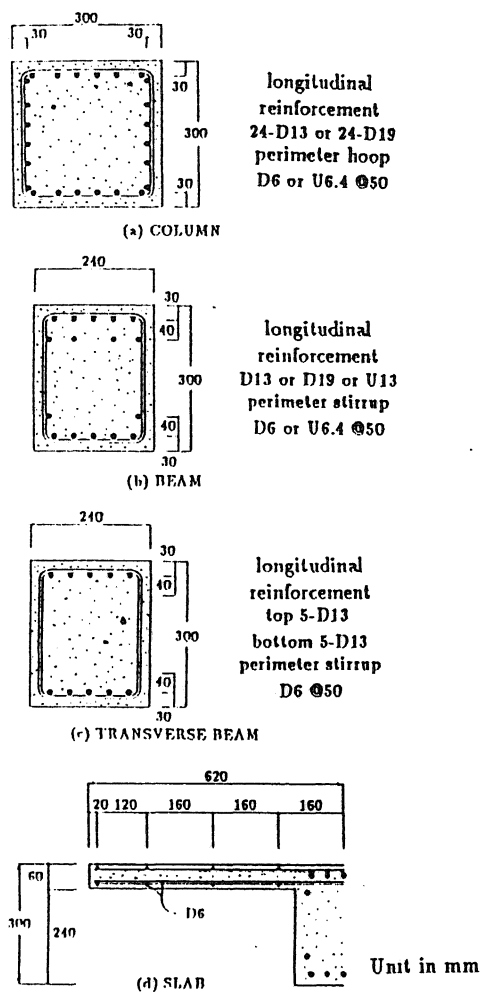


Figure 1 : Geometry of Specimens

ble 2 lists the reinforcement arrangement. Table 3 lists the mechanical properties of concrete and reinforcing steel. Deformed steel bar D13, and D19 and high strength steel rod with spiral grooves (U13) were used for longitudinal reinforcements. High strength deformed bars with yield strength larger than 500 MPa were special product for these tests. The longitudinal reinforcing bars were passed through the joints. For confinement of the joint core, five sets of high strength steel hoop (D6) were placed within the joint area. Three sets of hoops were used in specimen J-6 for a comparison. In the specimen J-3, twenty five transverse confining rods with diameter of 9.2 mm

Table 3 : Mechanical Properties of Concrete and Reinforcing Steel

(a) CONCRETE									
Specimen	J-1,2,3	J-4,5	J-6,7,8,9	J-10,11					
Compressive strength (MPa)	81.2	72.8	79.2	39.2					
Tensile split strength (MPa)	3.92	3.82	3.73	3.14					
Young's modulus (MPa)	$3.38 \times 10^4$	$3.95 \times 10^4$	$3.73 \times 10^4$	$3.07 \times 10^4$					
(b) REINFORCEMENT STEEL									
Specimen	J-1	J-2,3	J-4	J-5	J-6,7	J-8	J-9	J-10	J-11
Nominal sectional Area (mm <sup>2</sup> )	127	133	127	127	127	287	127	127	287
Nominal diameter (mm)	12.7	13.0	12.7	12.7	12.7	19.1	12.7	12.7	19.1
Yield strength (MPa)	638	1,456	515	839	676	370	676	700	372
Tensile strength (MPa)	808	1,517	650	902	860	532	860	933	545



**Figure 4 : Loading History**

were added in order to know the effect of extremely high confinement of joint core concrete. Sufficient transverse reinforcements necessary to prevent non-ductile failure were arranged for beams and columns.

### 2.3 Loading Program

Statically cyclic load was applied to failure maintaining constant thrust load to column. The loading setup for the tests is shown in Fig. 3. In order to simulate the condition in moment resisting frame subjected to earthquake lateral load, two servo-controlled hydraulic jacks were installed to pose vertical displacement to the two beams ends, while two columns ends were supported with lateral high-strength rods. Two beams was loaded by displacement control in opposite directions so that the vertical displacements were kept identical during the test. The distance between two loading points for beams and for columns were 2,860 mm and 1,400 mm respectively. Constant axial load; approximately, 15 % of column concrete compressive capacity was applied to column top by a hydraulic jack to simulate the gravity load in 3rd story column of 12 storied typical building. No load was applied to transverse beams or to slabs. The loading history is shown in Fig. 4. Basically two cycles with same amplitude of story drift angle were repeated then amplitude was increased.

## 2.4 Measurement

Beam end displacements and beam shear forces were measured. Story drift angle  $R$  is hereafter defined as Eq. (1).

$$R = (\delta_1 + \delta_2) / l_b \quad (1)$$

where,  $\delta_1, \delta_2$  : beam end displacements,  $l$  : distance between two loading points of beams (=2,860 mm).

Joint shear force  $V_j$  and joint shear stress  $\tau_j$  during tests were calculated as follows:

$$V_1 = V_{1b1} / j_1 + V_{2b2} / j_2 - V_c \quad (2)$$

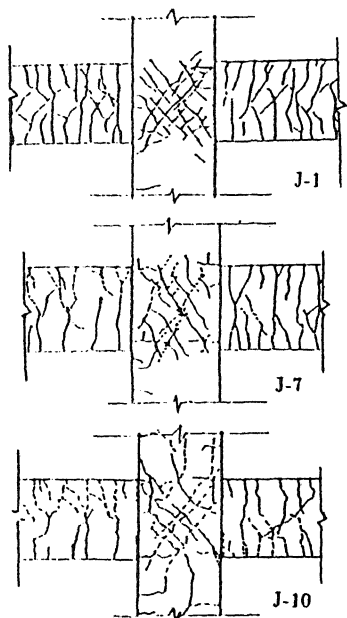


Figure 5 : Typical Crack Patterns

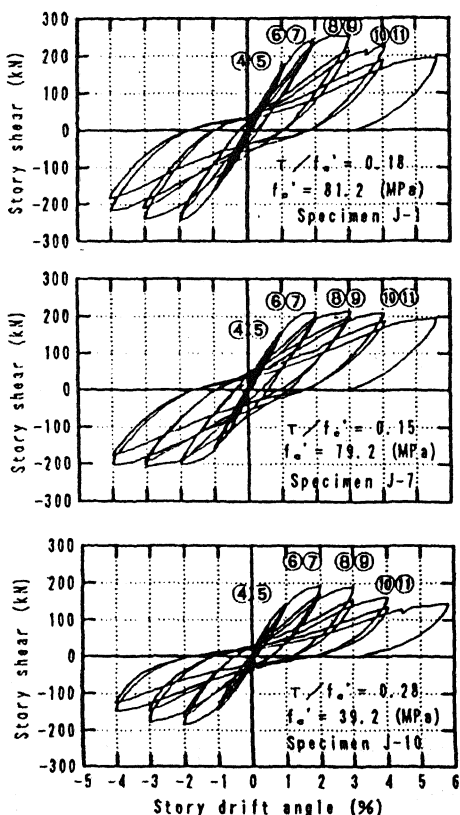


Figure 6 : Typical Story Shear-Story Drift Angle Relationship

$$\tau_j = V_j / A_j \quad (3)$$

where,  $V$  and  $V_c$  : beam shear,  $V$  : column shear,  $l_1$  and  $l_2$  : distance from column face to beam loading point (=1280 mm),  $j_1$  and  $j_2$  : distanced from tensile reinforcement to compressive resultant (assumed to be 243 mm), and  $A$  effective area of joint ( $= D (b + b_c) / 2$ ),  $D$  : column depth,  $b_c$  : column width,  $b$  : beam width.

### 3. TEST RESULTS

#### 3.1 Typical Sequence of Failure

Beam flexural cracks appeared and then diagonal shear cracks appeared on the joint surface. As increasing the story shear, the number of cracks increased. Figure 5 shows typical crack patterns at 2 % story drift. The crack spacing and crack patterns of high strength concrete specimens did not seem significantly different from that of conventional strength concrete specimen. Beam longitudinal bar yielded at approximately 2% of story drift angle. The story angle at which beam yielded increased as increasing the yield strength of beam longitudinal reinforcing bar.

#### 3.2 Hysteretic Behavior

Figure 6 shows typical story shear-story drift angle relationship for specimens of J-1, J-7 and J-10. Specimen J-1 and J-7 showed capability of steady dissipation of energy due to hysteresis loop and little strength degradation until the end of tests. However, specimen J-10 show sudden strength degradation due to joint shear failure prior to beam yieldings.

In order to quantify the energy dissipating capacity, equivalent viscous damping factors were calculated with respect to cycle. The viscous damping of second cycle of same amplitude was estimated 2 % to 5 % before beam yield and 5 % to 15 % after beam yield.

#### 3.3 Failure Modes

Specimens were classified according to observed sequence of beam yieldings and joint shear failure. The beam yieldings were judged from the strain gage readings on the beam longitudinal reinforcement. The first failure mode is "joint-shear failure prior to beams yielding (S)". Second one is "joint-shear failure after beam yield (FS)". The third one is "beam yield without joint shear failure (F)". Table 4 lists the failure mode, observed maximum story shear forces and shear stresses.

Table 4 : Observed Maximum joint shear and failure modes

Specimen	J-1	J-2	J-3	J-4	J-5	J-6	J-7	J-8	J-9	J-10	J-11
maximum story shear (kN)	257	276	286	265	297	274	219	311	294	196	232
maximum joint shear stress (MPa)	14.2	15.3	18.1	14.5	16.3	15.1	12.0	17.1	16.1	10.8	12.7
failure mode	FS	S	S	FS	S	FS	F	S <sup>1</sup>	F	S	S

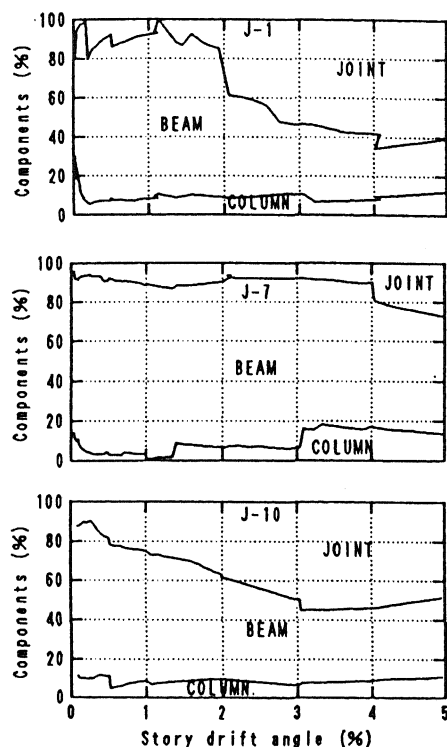


Figure 7 : Contributions towards Story Drift

### 3.4 Contributions towards Story Drift

Contributions of (1) deflection of beams (2) deflection of columns and (3) deflection of joint to the total inter-story drift are plotted against story drift angle in Fig. 7. As far as story drift angle was smaller than 0.5 %, the ratios of the contributions to total story drift were almost the same in three specimens. In case of specimens J-1 and J-7, 80 % of beams contribution was kept constant before story drift angle reached 2 %. In specimen J-10 the joint contribution increased gradually and reached approximately 50 % while the contributions of beams and columns decreased.

## 4. DISCUSSION

### 4.1 Effect of Concrete Compressive Strength to Ultimate Joint Shear

The concrete compressive strength is regarded as pri-

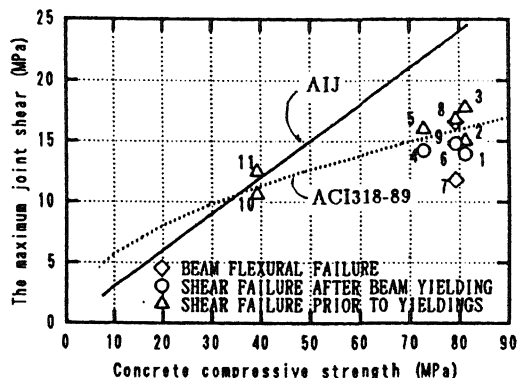


Fig. 8 : Relation of Concrete Compressive Strength and Observed Maximum Joint Shear

mary factor which affects the joint shear strength while the joint shear strength is not sensitive to the joint reinforcement in AIJ's guideline (1990). Therefore, the observed maximum joint shear calculated by Eq. (1) are plotted against concrete compressive strengths in Fig. 8 neglecting the difference in joint reinforcement. Six specimens (J-2, J-3, J-5, J-8, J-10, and J-11) failed in joint shear prior to beams yielding. It seemed that increase of horizontal joint shear capacity was not proportional to that of concrete compressive strength. The extrapolation of equation for joint shear in AIJ's guideline (1990) ( $\tau_j \geq 0.3 f'_c$ ) is shown in solid line, which assumes linear relation between joint shear strength and concrete compressive strength. It overestimates the test result in the range of concrete strength of 80 MPa. The ACI 318-89 recommendation ( $\tau_j \geq 15 \sqrt{f'_c}$  (in kips) for joints confined on two opposite faces (1989) is shown in dashed line and it well correlates with tests results of high-strength concrete specimen.

### 4.2 Effect of Reinforcement Ratio on Ultimate Joint Shear

The gross sectional area of longitudinal reinforcement also seemed to have an effect on joint shear capacity. The maximum joint shear of four specimens which failed in joint shear failure prior to beams yield are plotted against the beam tensile reinforcement ratio in Fig. 9. As increase the amount of tensile reinforcement, the observed joint shear capacity increased about 0 - 10 %. The fact that the one beam had al-

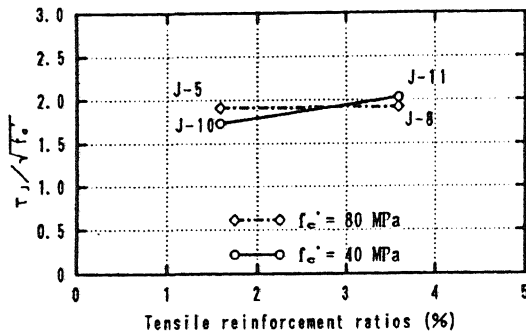


Fig. 9 : Relation of Beam Tensile Reinforcement Ratio and Observed Joint Shear Strength

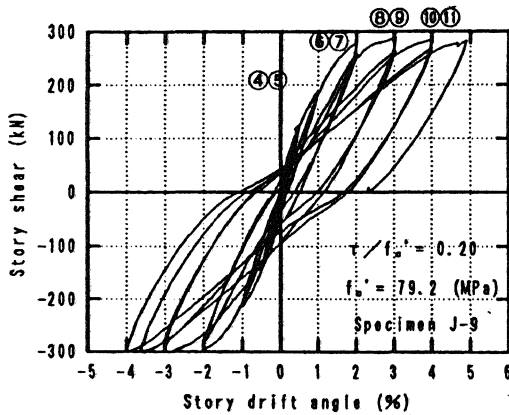


Figure 10 : Story Shear-Story Drift Angle Relationship of Specimen J-9

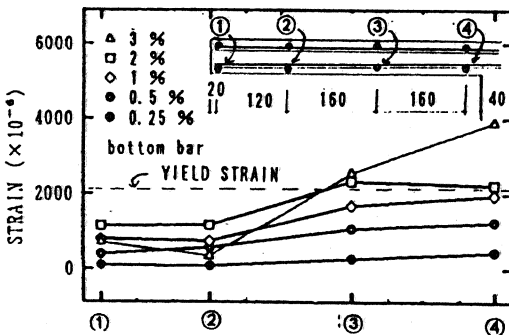


Figure 11 : Observed Strain in Slab Reinforcement at Slab-Transverse Beam Joint

ready yielded in specimen J-8, accounts for the reason why the joint shear J-8 show little increase in joint shear capacity compared with specimen J-11. Thus it is concluded that maximum joint shear is affected by amount of longitudinal reinforcement. It is unknown

whether beam or column reinforcement affect the joint shear strength.

### 4.3 Effect of Transverse Beams and Slab

Figure 10 shows the story drift angle-story shear relationship of the specimen J-9 which had transverse beams and a slab. It had no strength degradation and excellent hysteresis loop with much energy dissipation.

In order to know when the slab tensile reinforcement came into full effect for T-beam action, strains in slab bottom reinforcements parallel to the beams were measured by strain gages and distribution in a horizontal plain is shown in Fig. 11. At 2 % drift, the 80 % of the slab bottom reinforcements yielded. At 4 % drift, all of the slab reinforcements yielded.

## 5. CONCLUDING REMARKS

In order to evaluate the availability of current design provisions for interior beam-column-joint in high seismic regions, when applied to high strength concrete, Eleven 1/2.5 scale interior beam-column-joint subassemblages were made and subjected to statically cyclic loading to failure, maintaining constant axial load on column. The following concluding remarks are obtained from the tests.

1. The extrapolation of provisions for joint shear in AIJ recommendation, which assumes linear relation between joint shear strength and concrete compressive strength, overestimates the test result for high strength concrete higher than 40 MPa.
2. The ACI 318-89 recommendation shows good correlation with tests results of high-strength concrete specimen.
3. Maximum joint shear was affected by amount of longitudinal reinforcement. It is unknown whether beam or column reinforcement affect the result.

## ACKNOWLEDGMENT

This tests were conducted financially supported by a Building Research Institute, Japan. High strength steel bars were offered by Kozai-Club, Japan. Useful information and helpful advice of the members of Beam-Column-Joint and Frame Working Group under auspicious of New RC Project are greatly acknowledged.

Authors also wish to appreciate Mr. Toshiro Kawaguchi, KumagaiGumi Co. Ltd., Japan, Mr. Makoto Ogawara, Ohmoto-Gumi Co. Ltd. Japan, Mr. Jun Furukawa, TekkenKensetsu Co. Ltd., Japan and Mr. Tatsuro Satoh, Simiz Construction Co. Ltd., Japan, for

their cooperation in the tests and the task of compilation of tests data.

## REFERENCES

- ACI Committee 318, 1989, *Building Code Requirements for Reinforced Concrete (ACI 318-89)*, American Concrete Institute, pp. 353.
- Architectural Institute of Japan (AIJ) , 1990, *Design Guidelines for Earthquake Resistant Reinforced Concrete Buildings Based on Ultimate Strength Concept*, (in Japanese).
- Gilson N. Guimaraes, Michael E. Kreger, and James O. Jirsa , 1992, Evaluation of Joint-Shear Provisions for Interior Beam-Column-Slab Connections Using High-Strength Materials, *ACI Structural Journal*, V. 89, No. 1, Jan.-Feb., 89-98.